ELSEVIER

Seminars in
NUCLEAR
MEDICINE

Pitfalls on PET/CT Due to Artifacts and Instrumentation

Yu-Jung Tsai, PhD,* and Chi Liu, PhD*,†

PET/CT has become a preferred imaging modality over PET-only scanners in clinical practice. However, along with the significant improvement in diagnostic accuracy and patient throughput, pitfalls on PET/CT are reported as well. This review provides a general overview on the potential influence of the limitations with respect to PET/CT instrumentation and artifacts associated with the modality integration on the image appearance and quantitative accuracy of PET. Approaches proposed in literature to address the limitations or minimize the artifacts are discussed as well as their current challenges for clinical applications. Although the CT component can play an important role in assisting clinical diagnosis, we concentrate on the imaging scenarios where CT is used to provide auxiliary information for attenuation compensation and scatter correction in PET.
Semin Nucl Med 51:646-656

Introduction

The introduction of PET/CT allows the acquisition of both functional and anatomical information in a single imaging session.[1,2] It not only reduces the potential setup errors between separate CT and PET scans but also improves patient experience and throughput.[3,4] In current practice, PET/CT has been intensively applied in oncology, cardiology, and neurology. Its application is expected to expand further with the development of novel radioactive tracers.

Benefits of applying the integrated PET/CT in clinical practice have been evaluated in literature.[5] In terms of diagnostic accuracy, it has been demonstrated that PET/CT outperforms subsequent PET and CT studies viewed side-by-side.[6,7] The improvement is resulted from that both the image quality and quantitative accuracy of PET are improved as better attenuation correction[8] and scatter estimation[9] are achieved by incorporating information of the subject captured by CT.

This also encourages the exploration of potential clinical applications, such as disease followup,[10-13] therapy monitoring,[14-18] and receptor occupancy,[19,20] which rely on accurate quantification and object delineation on PET images. However, challenges emerge inevitably with the introduction of PET/CT in both clinical and research environment as well. The aim of this review is to provide a general overview on the current limitations with respect to PET/CT instrumentation and the image artifacts observed in PET/CT imaging. The possible solutions proposed in literature to address the limitations or eliminate the artifacts are discussed as well. Although, with the advancement of technology, the CT component of state-of-the-art PET/CT scanners is able to meet the clinical diagnostic merit and be used as a standalone CT scanner, this review focuses on discussion in imaging scenarios where CT is used to provide auxiliary information for PET.

Physics and Instrumentation of PET/CT

PET scanners are designed especially for positron-emitting radioactive tracers. When interacting with matter, the positron loses its kinetic energy and annihilates with an electron, creating two 511 keV photons emitted almost back-to-back. The travel range for a positron before it undergoes annihilation, named positron range, varies with the positron emitter applied. To capture these two photons, coincidence detectors positioned in opposite directions are used. Since one or both the photons may be scattered by any object along their travel to/in the detector, an energy discriminator can be used to

*Department of Radiology and Biomedical Imaging, Yale University, New Haven, CT.
†Department of Biomedical Engineering, Yale University, New Haven, CT.
The work of this review article is supported by NIH grants R01EB025468 and R01CA224140.
Address reprint requests to Chi Liu, PhD, Department of Radiology and Biomedical Imaging, Yale University, 330 Cedar St, New Haven, CT 06510. E-mail: chi.liu@yale.edu

 https://doi.org/10.1053/j.semnuclmed.2021.06.015
0001-2998/

prevent them being accepted in a wrong coincidence detector pair when the energy loss caused by the direction change is large enough. Given the annihilation can occur closer to one detector than the other, depending on the timing resolution of the detectors, two photons arriving a coincidence detector pair within a certain time window are registered as an event. The location of the annihilation can then be traced along the straight line defined by the paired coincidence detectors (line of response, LOR). For detectors with fine timing resolution, the difference in arrival time for the pair of annihilation photons (time-of-flight, TOF information) can be used to further reduce the location uncertainty of the event along the LOR.[21]

Current PET scanners usually adopt stationary detectors arranged in a ring shape to achieve 360-degree acquisition. Most PET detectors consist of scintillation crystals (scintillators) coupled with photosensors, such as photo-multiplier tubes and Silicon photo-multipliers for converting the energy of photon to electrical signals. To increase the efficiency of the conversion, thick scintillators can be chosen. However, due to the ring shape arrangement of detectors, this increases the probability of photons hitting on the side of scintillators, especially for annihilations occurring off the center of the field-of-view (FOV). These events can be slight mispositioned while estimating their location along the LOR when information regarding the depth of interaction in scintillators is not available.[22]

As annihilation photons can be absorbed (attenuated) by the imaging subject before interacting with the detector, the registered events will not reflect the true activity distribution in the subject. The attenuation rate depends on the photon energy as well as the distance and material that these photons have to travel through. In addition to provide anatomical information, CT can be used to estimate the attenuation as it is based on the variable absorption of x-rays by different tissues. A CT scanner consists of a donut-shape gantry, on which an x-ray tube and detectors positioned diametrically opposite to the tube are mounted. In contrast to the stationary geometry of PET, CT x-ray tube and detectors rotate simultaneously around the subject to achieve multiple angle acquisition. The voxel value in a CT image represents the linear attenuation coefficient of a given tissue in relation to that of water in Hounsfield Unit (HU). The noise level of a CT image is affected by the x-ray tube current and voltage. When a higher tube current or voltage is applied, more photons are generated and collected by the detectors hence a lower image noise level can be observed. The change of x-ray tube voltage also changes the CT image contrast as the attenuation rate of x-ray photon varies with its energy determined by the tube voltage. Since a typical CT x-ray tube generates photons with energy between 20 and 150 keV, the derived attenuation coefficients from a CT image have to be converted for photon energy of 511 keV for PET attenuation correction.[23]

Limitations With Respect to PET Instrumentation

As the purpose of the CT acquisition in most cases is to provide auxiliary information for PET, limitations with respect to PET/CT instrumentation can be focused on the system sensitivity and spatial resolution of PET scanners. The former quantifies the total efficiency of PET scanner to detect photons emitted from the subject while the later measures the capability of PET to distinguish close structures. It is well accepted that the diagnostic accuracy of PET is highly affected by these two factors as they determine the image quality and quantitative accuracy of the final PET images. In particular, low sensitivity of PET leads to high noise level in the images. This not only interferes the visual interpretation but also results in overestimation in applications based on quantitative analysis.[24] The image appearance is degraded in terms of object delineation by low spatial resolution as well. Since it is hard to obtain reliable regions-of-interests on the blurred images, the quantitative results derived from them can be biased.[25,26]

By increasing the system sensitivity, one can also achieve a higher patient throughput by shortening the imaging time[27] or a lower radiation exposure to both staff and patients by reducing the administered activity.[28,29] In terms of advanced application, it enables the performance of dynamic imaging with short time frames as well.[28,29] Many studies have shown that more information regarding the underlying physiological processes can be revealed by analyzing dynamic datasets.[30-35] Moreover, the increase of sensitivity also helps relieve the constraints on pursuing high resolution PET imaging.[36] For example, imaging configurations, such as narrow energy window, can be chosen to exclude small-angle scattering while maintaining reasonable count statistics.

In the past few decades, intensive efforts have been made in geometry and detector design to improve the sensitivity and resolution of PET scanners. For example, scanners with an extended axial FOV are developed to achieve ~5 to 40 times higher sensitivity than current commercial scanners for human whole-body studies [29,37-39] (Fig. 1). The introduction of detectors with small crystals and the ability of providing depth of interaction discrimination improves the localization of the pair of annihilation photons, which in turn improve the spatial resolution from ~3-5 mm to ~2-3 mm for ^{18}F-labeled human brain studies.[39] The system resolution can also be improved by adopting detectors with fine timing and energy resolution as a more accurate localization of photons and rejection of scattered events can be achieved. The innovations in PET instrumentation with respect to system and detector design are recently reviewed.[40]

Although advanced technical approaches, such as extremely long axial FOV and small crystals, are able to provide fundamental improvements in PET imaging, the implications to economics have limited most of their current applications within research purposes. Instead of pursuing high system spatial resolution of PET scanners, the effectiveness of incorporating TOF information and point spread function (PSF) that models the positron range of the applied positron emitter into a reconstruction algorithm to improve the spatial resolution and qualitative accuracy in the image domain has been demonstrated in literature.[41-51] However, since the modeling may involve high computational demand, the patient throughput could be affected accordingly.[52] In

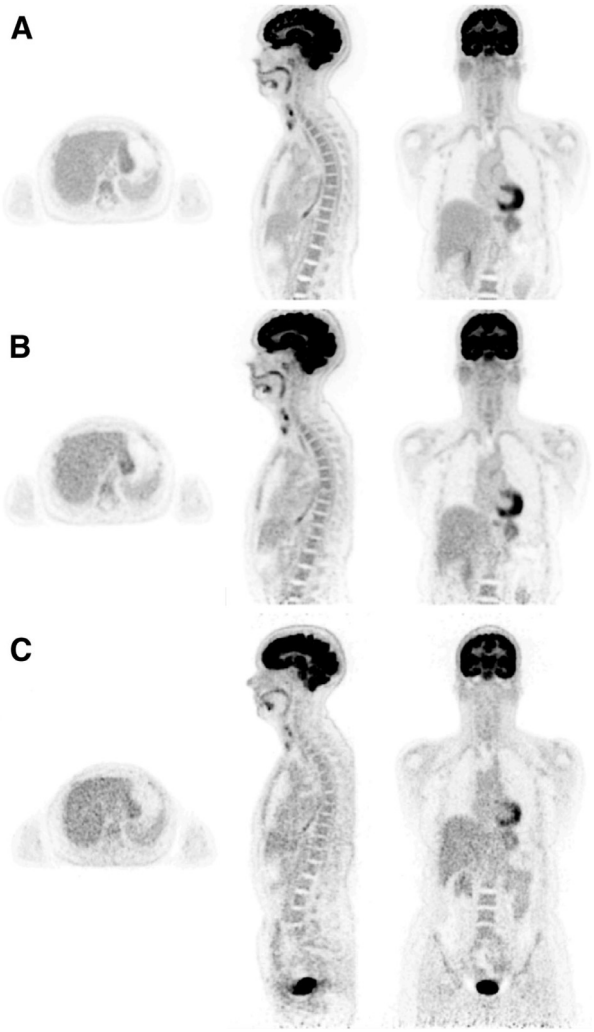

Figure 1 Representative axial (left), sagittal (middle) and coronal (right) views for a healthy subject imaged on the (A) PennPET Explorer (axial FOV = 64 cm) and (C) clinical Philips Ingenuity TF PET/CT (axial FOV = 18 cm) for 20 minutes. The PennPET Explore data were down sampled by 87.5% to represent a 2.5 minutes scan (B). The subject was injected with 555 MBq of ^{18}F-FDG and scanned at 1 and 1.5 hours after the injection on the Philips Ingenuity TF PET/CT and PennPET Explorer, respectively. An imaging protocol with 10 bed positions was conducted for the Philips Ingenuity TF PET/CT acquisition. Since the system sensitivity is improved as the axial FOV increases, the visual noise level for images in (B) is even lower than that for images in (C). (Adapted with permission from Ref 37.)

addition, it has been shown that PSF reconstruction could lead to edge artifacts at feature boundaries. For small lesion quantification, such artifacts could merge and form a "peak", resulting in overestimation of maximum standardized uptake value (SUV_{max}).[53] To modulate the influence of low system sensitivity on image noise level, a post filtering on the reconstructed images is often applied at the expense of image spatial resolution.[54,55] In recent years, deep learning based methods for image noise reduction have gained attention in research and clinical communities.[56-60] Although effective noise reduction can be achieved efficiently, images generated from these methods usually represent resolution loss. Moreover, the performance of the networks could depend on the noise level of the images used for training and vary with applications.[61]

Artifacts in PET/CT Imaging

Depending on the role of CT in PET data processing, different artifacts could emerge[62-64] Most artifacts observed in PET/CT imaging can be attributed to the misalignment between PET and CT data, errors in the CT-derived attenuation coefficients or CT image truncation.

Misalignment Between PET and CT Data

As the PET and CT data are usually obtained sequentially in practice, misalignment between these two datasets could happen due to motion of the subject between the acquisitions, and/or within either/both of the acquisitions. Even with careful positioning, good alignment between them could still be difficult to achieve as the time spans of the acquisitions is quite different.

The presence of misalignment between PET and CT images can lead to over/under estimation of regional activity distribution when the CT images are used for attenuation correction in PET[65-72] (Fig. 2). In the case where the CT data are utilized for scatter estimation, erroneous scatter estimation resulted from the misalignment could degrade the image quality significantly, rendering up the diagnostic value of PET[73,74] (Fig. 3). Literatures also show that deficiencies in scatter estimation can decrease the convergence rate of the applied iterative image reconstruction algorithm.[75] The

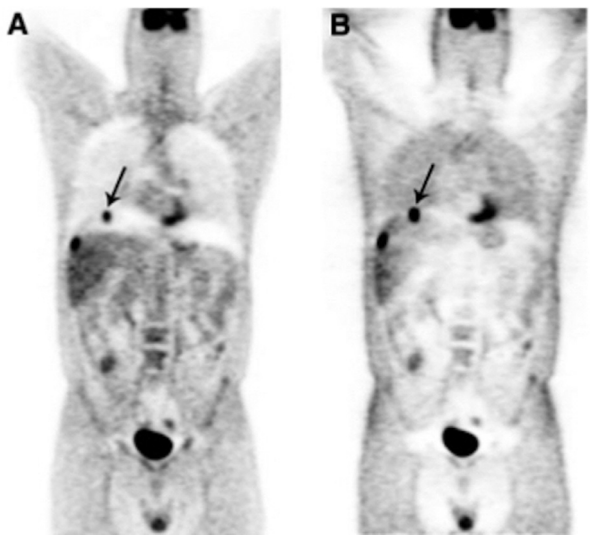

Figure 2 Representative coronal views for a subject with colon cancer. The PET data were reconstructed with (A) and without (B) applying the CT-based attenuation correction. The misalignment between PET and CT due to respiratory motion leads to curvilinear cold artifact around the lower lung and liver dome regions. The lesion at liver dome (indicated with an arrow) is mislocalized to right lung when the misaligned CT is used for attenuation correction. (Adapted with permission from Ref 64.)

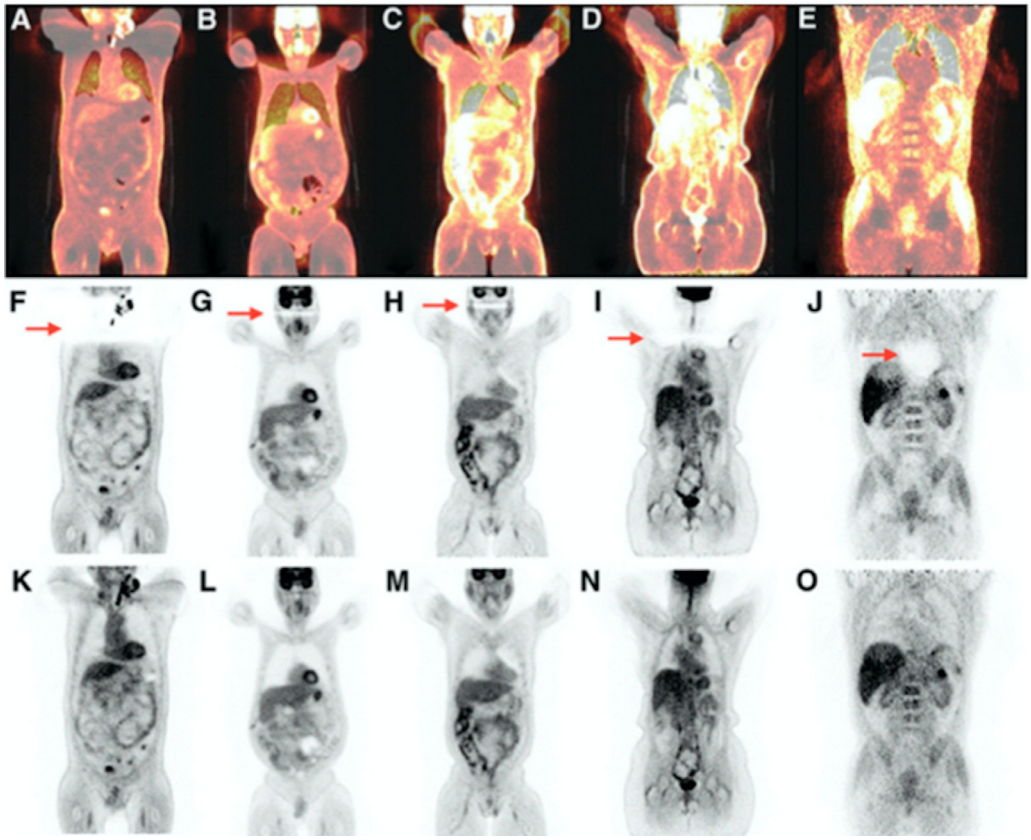

Figure 3 Representative coronal (right) views for five different patients showing artifacts resulted from arm motion.Each column shows data from different patient. First 4 columns show PET data obtained with ^{18}F-FDG (61 ± 16 minutes of uptake and 635 ± 67 MBq). Last column shows PET data obtained with ^{11}C-acetate (28 minutes of uptake and 639 MBq). The first row displays nonattenuation and scatter corrected PET images superimposed on the corresponding CT images to highlight the misalignment between PET and CT due to arm motion. PET images with CT-based attenuation and scatter correction are shown in the second row. Cold artifacts (indicated with red arrows) can be observed at the level of arm motion. The artifacts are substantially reduced (bottom row) by not applying scatter correction. (Adapted with permission from Ref 73.)

image quality and quantitative accuracy hence the diagnostic accuracy of PET can therefore be hampered by the over/under compensation for attenuation, erroneous scatter correction, slow algorithm convergence rate or any combination among them.

Although the diagnostic accuracy of PET can also be affected by the image blurry introduced by motion, this review concentrates on the image degradation factors resulted from the integration of PET and CT. In general, the motion effects that cause the misalignment issues in PET/CT can be categorized into two groups, voluntary motion and involuntary motion. The definition for each group of motion and the possible compensation strategies as well as their challenges in clinical applications will be discussed in this section.

Voluntary Motion

Voluntary motion refers to gross patient motion during and/or between the data acquisitions. In practice, the presence of voluntary motion can be limited by providing clear instruction to the patient. Cushions or holders that restrict movement of the patient can be applied as well.[62,72]

To tackle the misalignment caused by voluntary motion, software that performs image co-registration can be used to align the CT images with the PET images reconstructed without applying the CT-based attenuation correction. The outcome of the co-registration can then be utilized to transform the CT images which will later be incorporated into a final PET image reconstruction for attenuation correction and scatter estimation.[76,77] This two-step approach is straightforward and requires minimum changes to the applied reconstruction algorithm. However, it decreases the patient throughput due to the need of performing an additional PET reconstruction.

One strategy around the issue is to apply algorithms that simultaneously estimate the activity distribution and attenuation map from the PET data, leading to perfectly aligned attenuation correction as the attenuation map is derived from PET emission data.[78-81] The CT images are usually used to provide a priori knowledge regarding the intensity distribution of the attenuation map for the joint estimation as the problem is very ill-conditioned. The scattered events can be calculated based on the estimated attenuation map during the optimization as well. By exploring the information

contained in multiple energy windows, algorithms that allow joint estimation of activity distribution, attenuation map and scattered events are also proposed.[82] Although the influence of the misaligned CT images in PET reconstruction can be eliminated, the performance of these algorithms is sensitive to the data noise level and the availability of TOF information. In recent years, deep learning based methods are proposed to generate aligned attenuation maps[83-85] or directly the attenuation corrected PET images.[86] Networks that are able to achieve simultaneous attenuation and scatter correction are proposed as well.[87,88] This type of approaches is of great interest for clinical applications as it is able to generate the desired results much more efficient than other approaches once the network is trained. However, in addition to having access to powerful computation setups, a large scale PET/CT data collection is also essential for training the deep learning networks. Moreover, although promising results have been shown in literature, a thorough demonstration and evaluation for their reliability in different imaging applications are required.[89]

Involuntary Motion

Misalignment between PET and CT images induced by involuntary motion, including respiratory motion and cardiac contraction, is a well-known problem in PET/CT studies in the thorax region. Articles dedicating to the issue and its potential influence in practice can be found in literature.[90-95]

Given the time span of PET and CT acquisitions in practice, the reconstructed PET images represent the average position over multiple respiratory and cardiac cycles while the CT images acquired with only a few seconds typically under breath holding are snap shots capturing a nearly static position in the cycles. To eliminate the mismatch in position, CT scanning protocols that aim to obtain CT images representing the average respiratory/cardiac position can be employed.[96-100] As opposed to finding the averaged CT, methods based on respiratory/cardiac gating on both the CT and PET datasets are developed as well.[101-103] Depending on the applied gating techniques, the data are sorted into several gates according to the phase or displacement of the motion recorded using an external device or derived from the data themselves.[104] The gated CT and PET data are then paired up accordingly and either reconstructed individually and registered to a reference gate[105] or incorporated into 4-dimensional (4D) reconstruction algorithms.[106,107] Although satisfactory results are shown in literature, clinical applications of these methods are limited by the potential increase of patient total dose and decrease of patient throughput due to the need of special scans to obtain the averaged or gated CT images.

Assuming a finer phase or displacement sampling is applied and negligible motion effects in each gate of PET is observed, the misalignment problem between CT and each gate of PET can be treated as that caused by voluntary motion. Therefore, methods introduced in the previous section can also be utilized to achieve alignment between CT and each gate of PET.[108] Although sharing the same limitations as applied to voluntary motion, these approaches do not rely on the availability of the averaged or gated CT images. However, as only a portion of counts is included in each gate of PET, an additional image registration between a predefined reference gate and every other gate may be necessary to achieve preferable image noise level for visual interpretation. Instead of seeking the activity distribution and the corresponding attenuation map directly from the PET data, a different joint estimation algorithm incorporates a warp matrix into the objective function to take into account the smooth deformation between different gates induced by respiration and cardiac contraction.[109-111] Since the whole set of gated PET data is used for the optimization, this algorithm shows the potential to provide aligned attenuation map for each gate without increasing noise level. Similarly, the estimated scattered events can be updated using the deformed attenuation map during the optimization. Although the algorithm is less sensitive to data noise level, it is computationally expensive and shows dependency on the availability of TOF information.

In practice, respiratory motion is a more complicated issue than cardiac motion as the breathing pattern of the patient can change during and/or between the acquisitions. The performance of methods based on gated PET/CT datasets is therefore subject to the breathing variability and applied gating technique.[112-114] Although the dependency can be reduced by offering breathing coaching or controller during the scans.[115-118] regular breathing pattern throughout the data acquisitions is still hard to achieve, especially for patients with compromised lung function. To adapt to irregular breathing patterns, one strategy is to derive individual motion model from the nonattenuation corrected PET images to deform the CT images.[119] However, this approach requires initial PET reconstructions and shows performance dependence on tracer distribution and data statistics. The motion model can also be derived from CT images.[120-122] with the need of performing respiratory gated CT scans and risk failing when inconsistency in breathing pattern between the CT and PET acquisitions is observed. Although both the implications to imaging protocol and sensitivity to data statistics can be eliminated by using population-based motion models,[123,124] demonstrations on their usefulness in a clinical context are required. A thorough review on respiratory motion model development can be found in Ref 125.

Errors in CT-Derived Attenuation Coefficients

Contrast Medium

In practice, the conversion from CT numbers to attenuation coefficients for PET data correction is achieved by applying multilinear scaling methods. These methods generally work well with soft tissues and bone structures but could result in overestimation of attenuation for applications involving CT contrast agents.[126-131] This is because of that the contrast agents usually are designed to have high absorption rate for CT photon energies such that the underlying pathology can be enhanced in CT images. However, considering the difference in photon energies between PET and CT, the increase in

Figure 4 Representative coronal views for a subject with centrally located non−small cell cancer of right lung and mediastinal lymph node metastasis. Attenuation corrected PET image (A), PET/CT fusion image (B), CT image (C) and PET image uncorrected for attenuation (D) are given from left to right. The presence of highly concentrated contrast agent in right subclavian vein on CT image leads to erroneous attenuation correction in right axillary region (indicated with an arrow) on attenuation corrected PET. The hot spot is not detectable on PET image uncorrected for attenuation. (Adapted with permission from Ref 126.)

CT numbers caused by contrast agents may not correspond to a stronger attenuation effect in PET imaging. Therefore, the attenuation could be overestimated around the presence of contrast agent, leading to regional elevation of PET activity (Fig. 4). In addition to conducting a separate noncontrast CT for PET attenuation correction, scaling methods accounting for the influence of CT contrast agent[132,133] or photon energy difference between PET and CT[23] are proposed. The overestimation of attenuation can also be avoided by using negative oral contrast agents.[134] For applications where positive contrast agents are necessary, the injection concentration and protocol of the agent can be adjusted to reduce its influence on the derivation of attenuation coefficients.[135]

Metallic Implant

The other cause that leads to erroneous CT-derived attenuation coefficients is the presence of metal implants. Since the x-rays are mostly attenuated by the metallic objects, not much data are recorded in the projection bins intercepted with the implants. This results in dark and bright streaking artifacts after reconstruction of the data. Application of such CT images for PET attenuation correction introduces over/under estimation of tracer uptake in regions where the artifacts are observed (Fig. 5). This in turn biases quantification and visual interpretation of PET images. Various methods aiming to eliminate the streaking artifacts in CT images have been proposed. The majority of them involve distinguishing the values affected by the metallic objects and replacing them by appropriate estimates in the projection or image domain. There have also been approaches that incorporate estimation and correction of the artifacts into an image reconstruction algorithm. With potential increase of patient total dose, several studies suggest to eliminate the influence of the metallic implants by increasing the tube voltage of the CT scanner or employing a dual-energy CT scan. More details as well as the strengths and limitations of these strategies have been discussed in literature.[136-138] Recently, deep learning networks operating in the projection[139-141] or image domain[141-147] are also explode for achieving efficient metal artifact reduction.

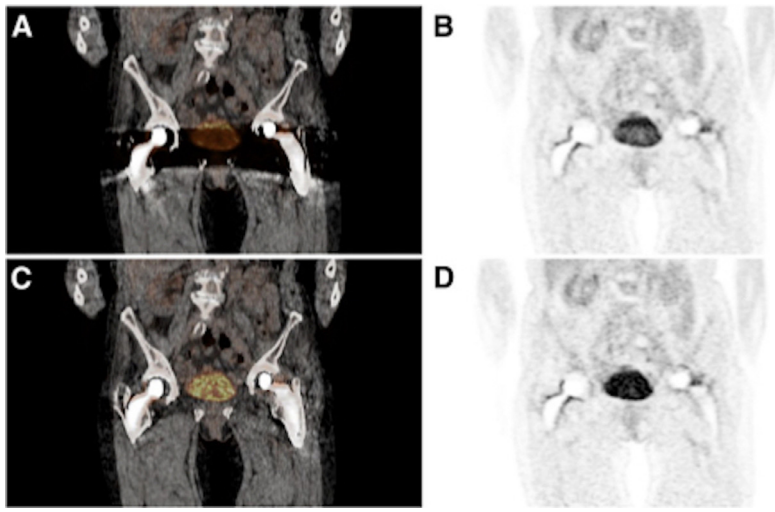

Figure 5 Representative coronal views for a subject with possible malignant cyst in right ovary. The metallic implants lead to a dark band in hip region on CT image (A). The artifact is substantially reduced by applying an iterative metal artifact reduction algorithm (C). PET images using CT without and with applying metal artifact reduction for attenuation correction are given in (B) and (D). The artifact in CT leads to lower activity in the corresponding regions on PET image. (Adapted with permission from Ref 149.)

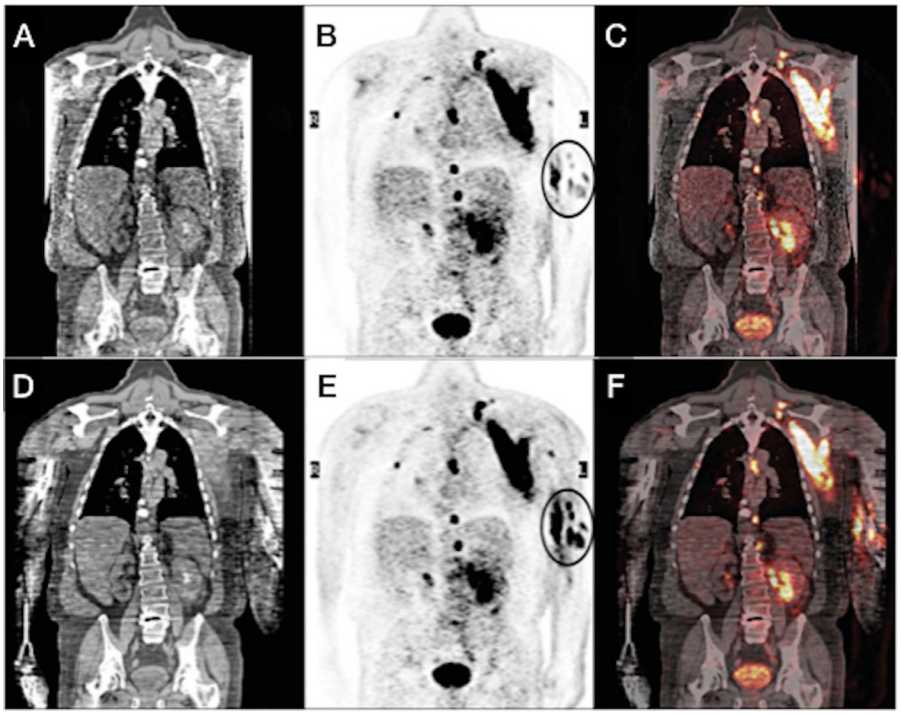

Figure 6 Representative coronal views for a subject with history of diffuse large B-cell lymphoma. The first row displays CT image with truncation of arms (A), PET image using the truncated CT for attenuation correction (B) and PET/CT fusion image. The corresponding results with truncation correction on CT are shown in the second row (D)-(F). The contrast of lesions within the truncated region becomes higher after applying the correction. In terms of quantification, an average difference of 328% in maximum standard uptake value (SUV) for four measurements of ^{18}F-FDG-avid tumor (within ellipse) was recorded. (Adapted with permission from Ref 153.)

Although most of the above mentioned methods are developed for diagnostic CT imaging, several studies have shown the effectiveness of considering metal artifact reduction techniques for PET/CT systems to prevent potential quantitative errors and false interpretation of PET images.[148-151]

CT Image Truncation

Since the transaxial FOV of CT is usually smaller than that of PET for commercial PET/CT systems, the anatomy covered in PET imaging could be truncated in CT, especially for large patients.[152] Different patient positioning in PET and CT acquisitions, for instance the arms of the patient are placed over the head in one scan but at the side in the other scan, can also lead to anatomy mismatch between PET and CT images. The lack of corresponding information from CT for attenuation correction can cause over-/underestimation of tracer concentration in PET[64] (Fig. 6). Although not being removed completely, issues induced by anatomy mismatch in PET and CT can be largely reduced by applying CT data extrapolation based on the assumption that the total attenuation of each projection should be a constant.[153-158] With small modifications, the algorithm proposed to estimate the attenuation map and activity distribution simultaneously can be used to estimate the missing attenuation information as well as the activity distribution.[158-159] However, as it requires an initial PET reconstruction and a priori information regarding the location of the affected regions, the algorithm shows potential implications to the patient throughput for clinical applications. Although further demonstration is required, a recently proposed machine learning based method can also be a possible solution.[160]

Conclusion

The introduction of combined PET/CT scanners has improved the diagnostic accuracy and patient throughput significantly in various fields. With decades of physics and instrumentation developments, potential clinical applications that rely on accurate lesion delineation and quantification have become possible. However, there are still technical challenges hence opportunities to make further improvement in PET/CT imaging to ensure that the best interests of both the health care providers and public are upheld.

References

1. Beyer T, Townsend DW, Brun T, et al: A combined PET/CT scanner for clinical oncology. J Nucl Med 41:1369-1379, 2000
2. Townsend DW, Cherry SR: Combining anatomy and function: The path to true image fusion. Eur Radiol 11:1968-1974, 2001
3. Townsend DW, Carney JPJ, Yap JT, et al: PET/CT today and tomorrow. J Nucl Med 45(suppl 1):4S-14S, 2004
4. Townsend DW, Beyer T: A combined PET/CT scanner: The path to true image fusion. Br J Radiol 75(suppl 9):S24-S30, 2002

5. Wechalekar K, Sharma B, Cook G: PET/CT in oncology-A major advance. Clin Radiol 60:1143-1155, 2005
6. Bar-Shalom R, Yefremov N, Guralnik L, et al: Clinical performance of PET/CT in evaluation of cancer: Additional value for diagnostic imaging and patient management. J Nucl Med 44:1200-1209, 2003
7. Lardinois D, Weder W, Hany TF, et al: Staging of non-small-cell lung cancer with integrated positron-emission tomography and computed tomography. N Engl J Med 348:2500-2507, 2003
8. Kinahan PE, Townsend DW, Beyer T, et al: Attenuation correction for a combined 3D PET/CT scanner. Med Phys 25:2046-2053, 1998
9. Watson CC, Casey ME, Michel C, et al: Advances in scatter correction for 3D PET/CT. Proc IEEE Nucl Sci Sym Med Imag Conf: 3008-3012, 2004
10. Ngeow JYY, Quek RHH, Ng DCE, et al: High SUV uptake on FDG-PET/CT predicts for an aggressive B-cell lymphoma in a prospective study of primary FDG-PET/CT staging in lymphoma. Ann Oncol 20:1543-1547, 2009
11. Sheikhbahaei S, Mena E, Yanamadala A, et al: The value of FDG PET/CT in treatment response assessment, follow-up, and surveillance of lung cancer. AJR Am J Roentgenol 208:420-433, 2017
12. Lewin J, Sayers L, Kee D, et al: Surveillance imaging with FDG-PET/CT in the post-operative follow-up of stage 3 melanoma. Ann Oncol 29:1569-1574, 2018
13. Marcus C, Marashdeh W, Ahn SJ, et al: 18F-FDG PET/CT and colorectal cancer: Value of fourth and subsequent posttherapy follow-up scans for patient management. J Nucl Med 56:989-994, 2015
14. Avril S, Muzic RF, Plecha D, et al: 18F-FDG PET/CT for monitoring of treatment response in breast cancer. J Nucl Med 57(Suppl 1):34S-39S, 2016
15. Ito K, Teng R, Schöder H, et al: 18F-FDG PET/CT for monitoring of ipilimumab therapy in patients with metastatic melanoma. J Nucl Med 60:335-341, 2019
16. Dimitrakopoulou-Strauss A: Monitoring of patients with metastatic melanoma treated with immune checkpoint inhibitors using PET-CT. Cancer Immunol Immunother 68:813-822, 2019
17. Ankrah AO, Span LFR, Klein HC, et al: Role of FDG PET/CT in monitoring treatment response in patients with invasive fungal infections. Eur J Nucl Med Mol Imaging 46:174-183, 2019
18. Barrington SF, Kluge R: FDG PET for therapy monitoring in Hodgkin and non-Hodgkin lymphomas. Eur J Nucl Med Mol Imaging 44(Suppl 1):S97-S110, 2017
19. Wang Y, Ayres KL, Goldman DA, et al: 18F-Fluoroestradiol PET/CT measurement of estrogen receptor suppression during a phase I trial of the novel estrogen receptor-targeted therapeutic GDC-0810: Using an imaging biomarker to guide drug dosage in subsequent trials. Clin Cancer Res 23:3053-3060, 2017
20. Lahesmaa M, Oikonen V, Helin S, et al: Regulation of human brown adipose tissue by adenosine and A2A receptors - Studies with [15O]H2O and [11C]TMSX PET/CT. Eur J Nucl Med Mol Imaging 46:743-750, 2019
21. Surti S: Update on time-of-flight PET imaging. J Nucl Med 56:98-105, 2015
22. Pizzichemi M, Stringhini G, Niknejad T, et al: A new method for depth of interaction determination in PET detectors. Phys Med Biol 61:4679-4698, 2016
23. Carney JPJ, Townsend DW, Rappoport V, et al: Method for transforming CT images for attenuation correction in PET/CT imaging. Med Phys 33:976-983, 2006
24. Lodge MA, Chaudhry MA, Wahl RL: Noise considerations for PET quantification using maximum and peak standardized uptake values. J Nucl Med 53:1041-1047, 2012
25. Boellaard R, Krak NC, Hoekstra OS, et al: Effects of noise, image resolution, and ROI definition on the accuracy of standard uptake values: A simulation study. J Nucl Med 45:1519-1527, 2004
26. Westerterp M, Pruim J, Oyen W, et al: Quantification of FDG PET studies using standardised uptake values in multi-centre trials: Effects of image reconstruction, resolution and ROI definition parameters. Eur J Nucl Med Mol Imaging 34:392-404, 2007
27. Watanabe M, Shimizu K, Omura T, et al: A high-throughput whole-body PET scanner using flat panel PS-PMTs. IEEE Trans Nucl Sci 51:796-800, 2004
28. Cherry SR, Jones T, Karp JS, et al: Total-body PET: Maximizing sensitivity to create new opportunities for clinical research and patient care. J Nucl Med 59:3-12, 2018
29. Surti S, Pantel AR, Karp JS: Total Body PET: Why, how, what for? IEEE Trans Radiat Plasma Med Sci 4:283-292, 2020
30. Dimitrakopoulou-Strauss A, Pan L, Sachpekidis C: Kinetic modeling and parametric imaging with dynamic PET for oncological applications: General considerations, current clinical applications, and future perspectives. Eur J Nucl Med Mol Imaging 48:21-39, 2021
31. Muzi M, O'Sullivan F, Mankoff DA, et al: Quantitative assessment of dynamic PET imaging data in cancer imaging. Magn Reson Imaging 30:1203-1215, 2012
32. Karakatsanis NA, Lodge MA, Tahari AK, et al: Dynamic whole-body PET parametric imaging: I. Concept, acquisition protocol optimization and clinical application. Phys Med Biol 58:7391-7418, 2013
33. Rahmim A, Lodge MA, Karakatsanis NA, et al: Dynamic whole-body PET imaging: principles, potentials and applications. Eur J Nucl Med Mol Imaging 46:501-518, 2019
34. Uprimny C, Kroiss AS, Decristoforo C, et al: Early dynamic imaging in 68Ga- PSMA-11 PET/CT allows discrimination of urinary bladder activity and prostate cancer lesions. Eur J Nucl Med Mol Imaging 44:765-775, 2017
35. Dimitrakopoulou-Strauss A, Pan L, Strauss LG: Quantitative approaches of dynamic FDG-PET and PET/CT studies (dPET/CT) for the evaluation of oncological patients. Cancer Imaging 12:283-289, 2012
36. Stickel JR, Cherry SR: High-resolution PET detector design: Modelling components of intrinsic spatial resolution. Phys Med Biol 50:179-195, 2004
37. Karp JS, Viswanath V, Geagan MJ, et al: PennPET explorer: Design and preliminary performance of a whole-body imager. J Nucl Med 61:136-143, 2020
38. Spencer BA, Berg E, Schmall JP, et al: Performance evaluation of the uEXPLORER total-body PET/CT scanner based on NEMA NU 2-2018 with additional tests to characterize long axial field-of-view PET scanners. J Nucl Med 62:861-870, 2021
39. Anton-Rodriguez JM, Julyan P, Djoukhadar I, et al: Comparison of a standard resolution PET-CT scanner with an HRRT brain scanner for imaging small tumors within the head. IEEE Trans Radiat Plasma Med Sci 3:434-443, 2019
40. Berg E, Cherry SR: Innovations in instrumentation for positron emission tomography. Semin Nucl Med 48:311-331, 2018
41. Prieto E, Domínguez-Prado I, García-Velloso MJ, et al: Impact of time-of-flight and point-spread-function in SUV quantification for oncological PET. Clin Nucl Med 38:103-109, 2013
42. Akamatsu G, Ishikawa K, Mitsumoto K, et al: Improvement in PET/CT image quality with a combination of point-spread function and time-of-flight in relation to reconstruction parameters. J Nucl Med 53:1716-1722, 2012
43. Akamatsu G, Mitsumoto K, Taniguchi T, et al: Influences of point-spread function and time-of-flight reconstructions on standardized uptake value of lymph node metastases in FDG-PET. Eur Radiol 83:226-230, 2014
44. Armstrong IS, Kelly MD, Williams HA, et al: Impact of point spread function modelling and time of flight on FDG uptake measurements in lung lesions using alternative filtering strategies. EJNMMI Phys 1:1-18, 2014
45. Armstrong IS, Tonge CM, Arumugam P: Impact of point spread function modeling and time-of-flight on myocardial blood flow and myocardial flow reserve measurements for rubidium-82 cardiac PET. J Nucl Cardiol 21:467-474, 2014
46. Presotto L, Gianolli L, Gilardi MC, et al: Evaluation of image reconstruction algorithms encompassing Time-Of-Flight and Point Spread Function modelling for quantitative cardiac PET: Phantom studies. J Nucl Cardiol 22:351-363, 2015
47. Schaefferkoetter J, Casey M, Townsend D, et al: Clinical impact of time-of-flight and point response modeling in PET reconstructions: A lesion detection study. Phys Med Biol 58:1465-1478, 2013
48. Lasnon C, Hicks RJ, Beauregard JM, et al: Impact of point spread function reconstruction on thoracic lymph node staging with 18F-FDG PET/CT in non-small cell lung cancer. Clin Nucl Med 37:971-976, 2012

49. Dasari PKR, Jones JP, Casey ME, et al: The effect of time-of-flight and point spread function modeling on 82Rb myocardial perfusion imaging of obese patients. J Nucl Cardiol 25:1521-1545, 2018
50. Lois C, Jakoby BW, Long MJ, et al: An assessment of the impact of incorporating time-of-flight information into clinical PET/CT imaging. J Nucl Med 51:237-245, 2010
51. Karp JS, Surti S, Daube-Witherspoon ME, et al: Benefit of time-of-flight in PET: Experimental and clinical results. J Nucl Med 49:462-470, 2008
52. Rahmim A, Qi J, Sossi V: Resolution modeling in PET imaging: Theory, practice, benefits, and pitfalls. Med Phys 40:064301, 2013
53. Alessio AM, Stearns CW, Tong S, et al: Application and evaluation of a measured spatially variant system model for PET image reconstruction. IEEE Trans Med Imag 29:938-949, 2010
54. Kim JH, Ahn IJ, Nam WH, et al: An effective post-filtering framework for 3-D PET image denoising based on noise and sensitivity characteristics. IEEE Trans Nucl Sci 62:137-147, 2015
55. Arabi H, Zaidi H: Improvement of image quality in PET using post-reconstruction hybrid spatial-frequency domain filtering. Phys Med Biol 63:215010, 2018
56. Lu W, Onofrey JA, Lu Y, et al: An investigation of quantitative accuracy for deep learning based denoising in oncological PET. Phys Med Biol 64:165019, 2019
57. Kaplan S, Zhu YM: Full-dose PET image estimation from low-dose PET image using deep learning: A pilot study. J Digit Imaging 32:773-778, 2019
58. Ladefoged CN, Hasbak P, Hornnes C, et al: Low-dose PET image noise reduction using deep learning: Application to cardiac viability FDG imaging in patients with ischemic heart disease. Phys Med Biol 66:054003, 2021
59. Domingues I, Pereira G, Martins P, et al: Using deep learning techniques in medical imaging: a systematic review of applications on CT and PET. Artif Intell Rev 53:4093-4160, 2020
60. Gong K, Guan J, Liu CC, et al: PET image denoising using a deep neural network through fine tuning. IEEE Trans Radiat Plasma Med Sci 3:153-161, 2019
61. Liu H, Wu J, Lu W, et al: Noise reduction with cross-tracer and cross-protocol deep transfer learning for low-dose PET. Phys Med Biol 65:185006, 2020
62. Corrigan AJ, Schleyer PJ, Cook GJ, et al: Pitfalls and artifacts in the use of PET/CT in oncology imaging. Semin Nucl Med 45:481-499, 2015
63. Bockisch A, Beyer T, Antoch G, et al: Positron emission tomography/computed tomography—Imaging protocols, artifacts, and pitfalls. Mol Imaging Biol 6:188-199, 2004
64. Sureshbabu W, Mawlawi O: PET/CT imaging artifacts. J Nucl Med Tech 33:156-161, 2005
65. Nordström J, Harms HJ, Kero T, et al: Effect of PET-CT misalignment on the quantitative accuracy of cardiac 15O-water PET. J Nucl Cardiol 2020. online access
66. Nekolla SG, Martinez-Möller A: Attenuation correction in cardiac PET: To raise awareness for a problem which is as old as PET/CT. J Nucl Cardiol 22:1296-1299, 2015
67. Rajaram M, Tahari AK, Lee AH, et al: Cardiac PET/CT misregistration causes significant changes in estimated myocardial blood flow. J Nucl Med 54:50-54, 2013
68. Tomita Y, Ishida M, Ichikawa Y, et al: The effect of misregistration between CT-attenuation and PET-emission images in 13N-Ammonia myocardial PET/CT. J Nucl Med Technol 44:73-77, 2016
69. Martinez-Möller A, Souvatzoglou M, Navab N, et al: Artifacts from misaligned CT in cardiac perfusion PET/CT studies: Frequency, effects, and potential solutions. J Nucl Med 48:188-193, 2007
70. Gould KL, Pan T, Loghin C, et al: Frequent diagnostic errors in cardiac PET/CT due to misregistration of CT attenuation and emission PET images: A definitive analysis of causes, consequences, and corrections. J Nucl Med 48:1112-1121, 2007
71. Lautamäki R, Brown TL, Merrill J, et al: CT-based attenuation correction in 82Rb-myocardial perfusion PET-CT: Incidence of misalignment and effect on regional tracer distribution. Eur J Nucl Med Mol Imaging 35:305-310, 2008
72. Lee TC, Alessio AM, Miyaoka RM, et al: Morphology supporting function: Attenuation correction for SPECT/CT, PET/CT, and PET/MR imaging. Q J Nucl Med Mol Imaging 60:25-39, 2016
73. Lodge MA, Mhlanga JC, Cho SY, et al: Effect of patient arm motion in whole-body PET/CT. J Nucl Med 52:1891-1897, 2011
74. Watson CC, Casey ME, Michel C, et al: Advances in scatter correction for 3D PET/CT. Proc IEEE Nucl Sci Sym Med Imag Conf: 3008-3012, 2004
75. Zaidi H, Montandon ML: Scatter compensation techniques in PET. PET Clin 2:219-234, 2007
76. Khurshid K, Berger KL, McGough RJ: Automated PET/CT brain registration for accurate attenuation correction. Annu Int Conf IEEE Eng Med Biol Soc: 5805-5808, 2009
77. Ye H, Wong K-P, Wardak M, et al: Automated movement correction for dynamic PET/CT images: Evaluation with phantom and patient data. PLoS ONE 9:e103745, 2014
78. Nuyts J, Dupont P, Stroobants S, et al: Simultaneous maximum a posteriori reconstruction of attenuation and activity distributions from emission sinograms. IEEE Trans Med Imag 18:393-403, 1999
79. Rezaei A, Defrise M, Bal G, et al: Simultaneous reconstruction of activity and attenuation in time-of-flight PET. IEEE Trans Med Imag 31:2224-2233, 2012
80. Rezaei A, Deroose CM, Vahle T, et al: Joint reconstruction of activity and attenuation in time-of-flight PET: A quantitative analysis. J Nucl Med 59:1630-1635, 2018
81. Li Y, Matej S, Karp JS: Practical joint reconstruction of activity and attenuation with autonomous scaling for time-of-flight PET. Phys Med Biol 65:235037, 2020
82. Brusaferri L, Bousse A, Emond EC, et al: Joint activity and attenuation reconstruction from multiple energy window data with photopeak scatter re-estimation in non-TOF 3-D PET. IEEE Trans Radiat Plasma Med Sci 4:410-421, 2019
83. Dong X, Wang T, Lei Y, et al: Synthetic CT generation from non-attenuation corrected PET images for whole-body PET imaging. Phys Med Biol 64:215016, 2019
84. Arabi H, Zaidi H: Deep learning-guided estimation of attenuation correction factors from time-of-flight PET emission data. Med Image Anal 64:101718, 2020
85. Hwang D, Kim KY, Kang SK, et al: Improving the accuracy of simultaneously reconstructed activity and attenuation maps using deep learning. J Nucl Med 59:1624-1629, 2018
86. Hu Z, Li Y, Zou S, et al: Obtaining PET/CT images from non-attenuation corrected PET images in a single PET system using Wasserstein generative adversarial networks. Phys Med Biol 65:215010, 2020
87. Dong X, Lei Y, Wang T, et al: Deep learning-based attenuation correction in the absence of structural information for whole-body positron emission tomography imaging. Phys Med Biol 65:055011, 2020
88. Mostafapour S, Gholamiankhah F, Dadgar H, et al: Feasibility of deep learning-guided attenuation and scatter correction of whole-body 68Ga-PSMA PET studies in the image domain. Clin Nucl Med 2021. online access
89. Lee JS: A review of deep-learning-based approaches for attenuation correction in positron emission tomography. IEEE Trans Radiat Plasma Med Sci 5:160-184, 2021
90. Goerres GW, Burger C, Kamel E, et al: Respiration-induced attenuation artifact at PET/CT: Technical considerations. Radiology 226:906-910, 2003
91. McQuaid SJ, Hutton BF: Sources of attenuation-correction artefacts in cardiac PET/CT and SPECT/CT. Eur J Nucl Med Mol Imaging 35:1117-1123, 2008
92. Schwaiger M, Ziegler S, Nekolla SG: PET/CT: Challenge for nuclear cardiology. J Nucl Med 46:1664-1678, 2005
93. Bacharach SL: PET/CT attenuation correction: Breathing lessons. J Nucl Med 4:677-679, 2007
94. Ghafarian P, Ay MR: The influence of PET and CT misalignment due to respiratory motion on the cardiac PET/CT imaging: A simulation study. Frontiers Biomed Technol 1:252-257, 2014
95. Sun T, Mok GS: Techniques for respiration-induced artifacts reductions in thoracic PET/CT. Quant Imaging Med Surg 2:46-52, 2012
96. Mok GSP, Ho CYT, Yang BH, et al: Interpolated average CT for cardiac PET/CT attenuation correction. J Nucl Cardiol 23:1072-1079, 2016

97. Chi PC, Mawlawi O, Nehmeh SA, et al: Design of respiration averaged CT for attenuation correction of the PET data from PET/CT. Med Phys 34:2039-2047, 2007
98. Pan T, Mawlawi O, Nehmeh SA, et al: Attenuation correction of PET images with respiration-averaged CT images in PET/CT. J Nucl Med 46:1481-1487, 2005
99. Alessio AM, Kohlmyer S, Branch K, et al: Cine CT for attenuation correction in cardiac PET/CT. J Nucl Med 48:794-801, 2007
100. Tzolos E, Lassen ML, Pan T, et al: Respiration-averaged CT versus standard CT attenuation map for correction of 18F-sodium fluoride uptake in coronary atherosclerotic lesions on hybrid PET/CT. J Nucl Cardiol 2020. online access
101. Nehmeh SA, Erdi YE: Respiratory motion in positron emission tomography/computed tomography: A review. Semin Nucl Med 38:167-176, 2008
102. Zhang R, Alessio AM, Pierce LA II, et al: Improved attenuation correction for respiratory gated PET/CT with extended-duration cine CT: A simulation study. Proc SPIE Med Imaging; Phys Med Imaging 2017:101321I
103. Nye JA, Esteves F, Votaw JR: Minimizing artifacts resulting from respiratory and cardiac motion by optimization of the transmission scan in cardiac PET/CT. Med Phys 34:1901-1906, 2007
104. Dawood M, Büther F, Lang N, et al: Respiratory gating in positron emission tomography: a quantitative comparison of different gating schemes. Med Phys 34:3067-3076, 2007
105. Nehmeh SA, Erdi YE, Pan T, et al: Four-dimensional (4D) PET/CT imaging of the thorax. Med Phys 31:3179-3186, 2004
106. Manjeshwar R, Tao X, Asma E, et al: Motion compensated image reconstruction of respiratory gated PET/CT. In: 3rd IEEE International Symposium on Biomedical Imaging:674-677, 2004
107. Qiao F, Pan T, Clark JW Jr, et al: A motion-incorporated reconstruction method for gated PET studies. Phys Med Biol 51:3769-3783, 2006
108. Hamill JJ, Panin VY: TOF-MLAA for attenuation correction in thoracic PET/CT. Proc IEEE Nucl Sci Sym Med Imag Conf: 4040-4047, 2012
109. Bousse A, Bertolli O, Atkinson D, et al: Maximum-likelihood joint image reconstruction/motion estimation in attenuation-corrected respiratory gated PET/CT using a single attenuation map. IEEE Trans Med Imag 35:217-228, 2016
110. Rezaei A, Michel C, Casey ME, et al: Simultaneous reconstruction of the activity image and registration of the CT image in TOF-PET. Phys Med Biol 61:1852-1874, 2016
111. Bousse A, Bertolli O, Atkinson D, et al: Maximum-likelihood joint image reconstruction and motion estimation with misaligned attenuation in TOF-PET/CT. Phys Med Biol 61:L11-L19, 2016
112. Qi W, Ponce S, Xia T, et al: Investigation of phase and amplitude respiratory gating for whole-body FDG-PET with different respiratory waveform patterns. Nucl Med Commun 57(suppl 2):1892, 2016
113. Tsutsui Y, Kidera D, Taniguchi T, et al: Accuracy of amplitude-based respiratory gating for PET/CT in irregular respirations. Ann Nucl Med 28:770-779, 2014
114. Liu C, Pierce LA 2nd, Alessio AM, et al: The impact of respiratory motion on tumor quantification and delineation in static PET/CT imaging. Phys Med Biol 54:7345-7362, 2009
115. Gilman MD, Fischman AJ, Krishnasetty V, et al: Optimal CT breathing protocol for combined thoracic PET/CT. AJR Am J Roentgenol 187:1357-1360, 2006
116. Changlai SP, Huang CK, Luzhbin D, et al: Using cine-averaged CT with the shallow breathing pattern to reduce respiration-induced artifacts for thoracic cavity PET/CT scans. AJR Am J Roentgenol 213:140-146, 2019
117. Sun T, Wu TH, Wang SJ, et al: Low dose interpolated average CT for thoracic PET/CT attenuation correction using an active breathing controller. Med Phys 40:102507, 2013
118. Nehmeh SA, Erdi YE, Meirelles GS, et al: Deep-inspiration breath-hold PET/CT of the thorax. J Nucl Med 48:22-26, 2007
119. Kalantari F, Wang J: Attenuation correction in 4D-PET using a single-phase attenuation map and rigidity-adaptive deformable registration. Med Phys 44:522-532, 2017
120. McClelland JR, Blackall JM, Tarte S, et al: A continuous 4D motion model from multiple respiratory cycles for use in lung radiotherapy. Med Phys 33:3348-3358, 2006
121. Ehrhardt J, Werner R, Säring D, et al: An optical flow based method for improved reconstruction of 4D CT data sets acquired during free breathing. Med Phys 34:711-721, 2007
122. McClelland JR, Hughes S, Modat M, et al: Inter-fraction variations in respiratory motion models. Phys Med Biol 56:251-272, 2011
123. Kalantari F, Wang J: Attenuation correction in 4D-PET using a single-phase attenuation map and rigidity-adaptive deformable registration. Med Phys 44:522-532, 2017
124. McQuaid SJ, Lambrou T, Hutton BF: A novel method for incorporating respiratory-matched attenuation correction in the motion correction of cardiac PET-CT studies. Phys Med Biol 56:2903-2915, 2011
125. McClelland JR, Hawkes DJ, Schaeffter T, et al: Respiratory motion models: a review. Med Image Anal 17:19-42, 2013
126. Antoch G, Freudenberg LS, Egelhof T, et al: Focal tracer uptake: a potential artifact in contrast-enhanced dual-modality PET/CT scans. J Nucl Med 43:1339-1342, 2002
127. Antoch G, Freudenberg LS, Beyer T, et al: To enhance or not to enhance? 18F-FDG and CT contrast agents in dual-modality 18F-FDG PET/CT. J Nucl Med 45(suppl 1):56S-65S, 2004
128. Mawlawi O, Erasmus JJ, Munden RF, et al: Quantifying the effect of IV contrast media on integrated PET/CT: clinical evaluation. AJR Am J Roentgenol 186:308-319, 2006
129. Visvikis D, Costa DC, Croasdale I, et al: CT-based attenuation correction in the calculation of semi-quantitative indices of [18F]FDG uptake in PET. Eur J Nucl Med 30:344-353, 2003
130. Cronin CG, Prakash P, Blake MA: Oral and IV contrast agents for the CT portion of PET/CT. AJR Am J Roentgenol 195:W5-W13, 2010
131. Dizendorf E, Hany TF, Buck A, et al: Cause and magnitude of the error induced by oral CT contrast agent in CT-based attenuation correction of PET emission studies. J Nucl Med 44:732-738, 2003
132. Büther F, Stegger L, Dawood M, et al: Effective methods to correct contrast agent-induced errors in PET quantification in cardiac PET/CT. J Nucl Med 48:1060-1068, 2007
133. Nehmeh SA, Erdi YE, Kalaigian H, et al: Correction for oral contrast artifacts in CT attenuation-corrected PET images obtained by combined PET/CT. Humm J Nucl Med 44:1940-1944, 2003
134. Antoch G, Kuehl H, Kanja J, et al: Dual-modality PET/CT scanning with negative oral contrast agent to avoid artifacts: introduction and evaluation. Radiology 230:879-885, 2004
135. Beyer T, Antoch G, Bockisch A, et al: Optimized intravenous contrast administration for diagnostic whole-body 18F-FDG PET/CT. J Nucl Med 46:429-435, 2005
136. Abdoli M, Mehranian A, Ailianou A, et al: Assessment of metal artifact reduction methods in pelvic CT. Med Phys 43:1588, 2016
137. Gjesteby L, Man BD, Jin Y, et al: Metal artifact reduction in CT: Where are we after four decades? IEEE Access 4:5826-5849, 2016
138. Wellenberg RHH, Hakvoort ET, Slump CH, et al: Metal artifact reduction techniques in musculoskeletal CT-imaging. Eur J Radiol 107:60-69, 2018
139. Ghani MU, Karl WC: Fast enhanced CT metal artifact reduction using data domain deep learning. IEEE Trans Comput Imag 6:181-192, 2020
140. Hegazy MAA, Cho MH, Cho MH, et al: U-net based metal segmentation on projection domain for metal artifact reduction in dental CT. Biomed Eng Lett 9:375-385, 2019
141. Arabi H, Zaidi H: Deep learning-based metal artefact reduction in PET/CT imaging. Eur Radiol 2021. online access
142. Gjesteby L, Yang Q, Xi Y, et al: Deep learning methods for CT image-domain metal artifact reduction. Proc SPIE Deven X-Ray Tomograp XI 2017:103910W
143. Xu S, Dang H: Deep residual learning enabled metal artifact reduction in CT. Proc SPIE Med Imaging; Phys Med Imaging 2018:105733O
144. Zhang Y, Yu H: Convolutional neural network based metal artifact reduction in X-Ray computed tomography. IEEE Trans Med Imag 37:1370-1381, 2018

145. Liao H, Lin WA, Zhou SK, et al: ADN: Artifact disentanglement network for unsupervised metal artifact reduction. IEEE Trans Med Imag 39:634-643, 2020
146. Zhang Y, Chu Y, Yu H: Reduction of metal artifacts in x-ray CT images using a convolutional neural network. Proc SPIE Dev X-Ray Tomography XI 2017:103910V
147. Huang X, Wang J, Tang F, et al: Metal artifact reduction on cervical CT images by deep residual learning. Biomed Eng Online 17:175, 2018
148. Abdoli M, Dierckx RA, Zaidi H: Metal artifact reduction strategies for improved attenuation correction in hybrid PET/CT imaging. Med Phys 39:3343-3360, 2012
149. van der Vos CS, Arens AIJ, Hamill JJ, et al: Metal artifact reduction of CT scans to improve PET/CT. J Nucl Med 58:1867-1872, 2017
150. Martin O, Aissa J, Boos J, et al: Impact of different metal artifact reduction techniques on attenuation correction in 18F-FDG PET/CT examinations. Br J Radiol 93, 2020
151. Schabel C, Gatidis S, Bongers M, et al: Improving CT-based PET attenuation correction in the vicinity of metal implants by an iterative metal artifact reduction algorithm of CT data and its comparison to dual-energy-based strategies: A phantom study. Invest Radiol 52:61-65, 2017
152. Habing R, Oliver D, Botkin C, et al: Patterns and prevalence of truncation artifacts in PET/CT. J Nucl Med 50(suppl 2):2227, 2009
153. Mawlawi O, Erasmus JJ, Pan T, et al: Truncation artifact on PET/CT: Impact on measurements of activity concentration and assessment of a correction algorithm. AJR Am J Roentgenol 186:1458-1467, 2006
154. Beyer T, Bockisch A, Kühl H, et al: Whole-body 18F-FDG PET/CT in the presence of truncation artifacts. J Nucl Med 47:91-99, 2006
155. Hsieh J, Chao E, Thibault J, et al: A novel reconstruction algorithm to extend the CT scan field-of-view. Med Phys 31:2385-2391, 2004
156. Sourbelle K, Kachelriess M, Kalender WA: Reconstruction from truncated projections in CT using adaptive detruncation. Eur Radiol 15:1008-1014, 2005
157. Zamyatin AA, Nakanishi S: Extension of the reconstruction field of view and truncation correction using sinogram decomposition. Med Phys 34:1593-1604, 2007
158. Nuyts J, Bal G, Kehren F, et al: Completion of a truncated attenuation image from the attenuated PET emission data. IEEE Trans Med Imag 32:237-246, 2013
159. Zhu W, Feng T, Dong Y, et al: A reliable PET data-based method for truncation compensation in quantitative PET/CT and PET/MR. J Nucl Med 58(suppl 1):697, 2017
160. Chen Y, Budde A, Li K, et al: A platform-independent method to reduce CT truncation artifacts using discriminative dictionary representations. Med Phys 44:121-131, 2017.